Photochemistry and Photobiology, 20**, **: *–*

Photochemical and Thermal Stability of Some Dihydroxyacetophenones Used as UV-MALDI-MS Matrices†

Olga I. Tarzi[1], Luciano Di Stéfano[1], Juan E. Argüello*[2], Gabriela Oksdath-Mansilla[2] and Rosa Erra-Balsells*[1]

[1]CIHIDECAR-CONICET, Departamento de Quimica Organica, Facultad de Ciencias Exactas y Naturales, Universidad de Buenos Aires, Ciudad Universitaria, Buenos Aires, Argentina
[2]INFIQC, Departamento de Quimica Organica, Facultad de Ciencias Quimicas, Universidad Nacional de Cordoba, Ciudad Universitaria, Cordoba, Argentina

Received 16 March 2013, accepted 27 June 2013, DOI: 10.1111/php.12130

ABSTRACT

2,4-, 2,5-, 2,6- and 3,5-dihydroxyacetophenone (DHA) used as matrices in matrix-assisted ultraviolet laser desorption/ionization mass spectrometry (UV-MALDI-MS) were studied by steady-state and transient absorption spectroscopy, together with DFT calculations at the B3LYP level of theory. All compounds have low fluorescence quantum yields, possibly due to an efficient excited-state intramolecular proton transfer (ESIPT). Laser flash photolysis (LFP) results showed that, only for 2,4-DHA, a phototautomer could be detected at λ = 400 nm. Their photochemical stability in solution at different wavelengths and conditions was analyzed by UV–Vis and ^{1}H nuclear magnetic resonance spectroscopy (^{1}H-NMR), together with thin layer chromatography and ultraviolet laser desorption/ionization mass spectrometry (UV-LDI-MS). Only 3,5-DHA showed decomposition when irradiated, probably because phototautomerization is not possible. Thermal stability studies of these compounds in solid state were also conducted.

INTRODUCTION

One of the most successful applications of organic photochemistry in solid state is UV-MALDI mass spectrometry. Through this analytical technique, desorption/ionization of the analyte is induced by a UV laser and assisted by a photosensitizer (matrix). Although the standard compounds used as matrices in UV-MALDI-MS are commercial, most of their photochemical properties remain unknown and there is not yet a clear model for the photosensitized process that takes place from the matrix to the analyte, after the UV-laser shot. In addition, no rules are followed when it comes to choosing the right matrix for a particular analyte. Knowing which properties photosensitizers should have to efficiently desorb the analyte could help to simplify the UV-MALDI experiment and to obtain new structures useful as matrices.

In 1995, Mohr *et al.* (1) introduced 2,6-dihydroxyacetophenone as a matrix in UV-MALDI-MS to analyze several oligosaccharides. Since then, dihydroxyacetophenones, particularly 2,4, 2,5 and 2,6- isomers, have been widely used as UV-MALDI matrices for peptides and carbohydrates (2–4). Experiments performed in our laboratory showed that also 3,5-DHA can desorb several oligosaccharides (see example in Supplementary Materials, Figure S1). However, no complete comparison of the four isomers has been informed in the literature. Krause *et al.* (2) studied 2,4, 2,5, 2,6 and 3,5-DHA as UV-MALDI matrices and found that the last one was unable to desorb the analytes used; yet, they did not discuss the reason for the difference in efficiency that the other three photosensitizers showed in their study. It is well known that *ortho*-hydroxybenzoyl compounds undergo a fast intramolecular hydrogen atom transfer reaction at the first excited single state, with a large Stokes shift (5–7). Although Krause *et al.* (2) suggested that the intramolecular proton transfer in 2,4-, 2,5- and 2,6-dihydroxyacetophenone is may be responsible for their ability to desorb the analyte when used as matrices in UV-MALDI experiments, no comprehensive studies involving the photochemistry and photophysics of these compounds were reported. Lüdeman *et al.* (8) only gave a very brief description of the transient absorption spectrum of 2,5-DHA, but did not study the other position isomers.

Regarding thermal stability, Ehring *et al.* (9) studied the photochemical *versus* thermal mechanisms in UV-MALDI-MS using 2,5-dihydroxybenzoic acid as matrix, but they did not take into account the thermochemical stability of the compounds involved in the UV-MALDI process, although they suggested, as a conclusion, that most of the energy is converted into matrix heating following photoexcitation (10). Knowledge of the thermal stability and possible high-temperature-induced chemical reactions of the common UV-MALDI matrices should play a critical role in understanding why some matrices are "highly" resistant to laser shots during the experiments, whereas, for others, after a few shots on the same sweet spot, the ion signal vanishes, preventing the detection of the intact analyte molecular ion (3,11). In view of this, Tarzi *et al.* (12) examined, form a chemical point of view, the thermal stability of different classical matrices such as 2,5-dihydroxybenzoic acid, 2,4,6-trihydroxyacetophenone, α-cyano-4-hydroxycinnamic acid, 3,5-dimethoxy-4-hydroxycinnamic acid, nor-harmane and harmane.

In this study, we focused our attention on a series of dihydroxyacetophenones indicated in Fig. 1. We used steady-state as well as transient absorption spectroscopy to investigate

*Corresponding author emails: erra@qo.fcen.uba.ar (Rosa Erra-Balsells); jea@fcq.unc.edu.ar (Juan E. Argüello)
†This article is part of the Special Issue dedicated to the memory of Elsa Abuin.

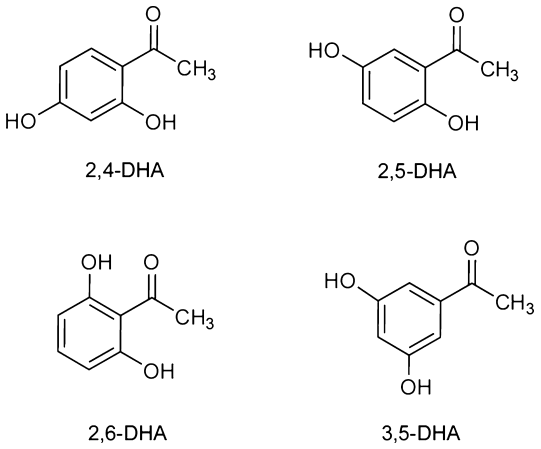

Figure 1. Structure of the dihydroxyacetophenones studied.

the excited states of these compounds. Although MALDI measurements are conducted in solid state; to begin with the study of the photochemistry (photochemical stability and photophysics) of compounds used as MALDI matrixes in solution is a proper starting point. The thermal stability of the selected matrices at their melting point was also studied, using different tools such as frontal ratio (F_r; thin layer chromatography, TLC), UV-absorption spectroscopy, ^{1}H nuclear magnetic resonance spectroscopy (^{1}H-NMR) and ultraviolet laser desorption/ionization time-of-flight mass spectrometry (UV-LDI-TOF-MS), for monitoring the remaining material obtained after heating. Dihydroxyacetophenones showed thermal stability in the experimental conditions and were recovered unchanged after melting experiments, except for 3,5-DHA that showed darkening of the product. They were also recovered unchanged after 100–200 shots by the UV laser in UV-LDI-MS experiments conducted in a laser desorption/ionization mass spectrometer with a Nd: YAG laser source (λ_{exc} = 355 nm).

MATERIALS AND METHODS

Chemicals. Dihydroxyacetophenones were purchased from Sigma-Aldrich Chemicals Co. (Milwaukee) Acetonitrile, methanol, ethanol, isopropanol, *tert*-butanol and 1,3-propanediol (Merck HPLC grade) were used as purchased, without any further purification. Deuterated solvents (Merck, Darmstadt, Germany) were high-quality PA grade. Sulfuric acid of analytical grade was used. Water was filtered Milli-Q purity. Quinine sulfate (QS; Aldrich Chemicals Co.) was used as purchased. Calibrant chemicals for UV-MALDI-MS nor-harmane (m. w. 168.068 Da) and β-cyclodextrin (m. w. 1135.0 Da) were purchased from Sigma-Aldrich (Milwaukee). 1^F-fructofuranosylnystose (m. w. 828.28 Da) was purchased from Wako Pure Chemical Industries (Osaka, Japan).

Electronic spectroscopy and photophysical experiments. Absorption measurements were performed with a UV–Visible spectrophotometer Shimadzu UV-1203. The spectrofluorimeter employed in this study was a PTI QM-1 Quanta Master whose output is automatically corrected for instrumental response by means of a Rhodamine B quantum counter and equipped with a Xe lamp and a Hamamatsu photomultiplier. Steady-state spectra were obtained in freshly prepared air-saturated and in Ar-saturated solution.

Fluorescence quantum yields (Φ_f) were determined at room temperature, relative to QS (10^{-5} M in H_2SO_4 1 *N*), Φ_f = 0.595 (13,14). The excitation wavelength was set to 355 nm and the monochromator slits to 2.5 nm. The diluted reference and samples were optically matched ($A < 0.1$). Corrections were made for difference in refractive index as well as for emission spectra.

Laser Flash Photolysis (LFP). Transient absorption spectra and quenching were determined using a Continuum-Surelite I Nd:YAG laser generating 355 nm laser pulse (10 mJ per pulse, *ca* 10 ns pulse duration) as excitation source. The spectrometer was a commercial Applied Photophysics, LKS80. All the kinetic determinations were performed at 25 ± 1°C.

^{1}H-NMR spectra were registered on a Bruker AC-200 (200 MHz) spectrometer. Chemical shifts (δ) are reported in parts per million (ppm), relative to internal tetramethylsilane. Measurements were carried out using the standard pulse sequences. The deuterated solvent used is indicated in each case.

UV-LDI-MS. Ultraflex II MALDI-TOF/TOF (Bruker Daltonics), with a Nd: YAG laser (λ_{exc} = 355 nm) as excitation source. Compounds were measured in positive and negative linear modes using 10^{-2}–10^{-3} M matrix concentration and 10^{-3} M analyte concentration in CH_3OH:H_2O 1:1 (v:v) and CH_3CN:H_2O 1:1 (v:v). Matrix stock solutions were made by dissolving 5 mg of the selected compound in 0.2 mL of MeOH–H_2O (1:1, v/v) or in 0.2 mL of MeCN–H_2O (2:3, v/v). Calibration was performed with *nor*-harmane (m. w. 168.068 Da) and β-cyclodextrin (m .w. 1135.0 Da) using the FlexControl software.

Photochemical stability experiments. Acetonitrile DHA solutions (10^{-4} M) were irradiated at room temperature under stirring and in air or nitrogen atmosphere, in 1 cm stoppered quartz cuvettes using three fluorescent tubes of 254 or 366 nm (Osram, 18 W each one). A Heraeus TQ 150-Z3, 150 Watt lamp, water cooled through a Pyrex jacket was also used (λ_{exc} > 300 nm). Experiments were monitored by TLC, UV–Vis and ^{1}H-NMR spectroscopy and UV-LDI-MS. Preparative irradiations were performed in a similar way, using quartz Erlenmeyers and 5×10^{-3} M acetonitrile solutions. TLC analysis was performed with aluminum silica gel sheets (0.2 layer thickness, silica gel 60 F254, Merck). The spots were visualized by UV light (λ_{exc} = 254 nm) or I_2 vapors.

Thermal stability experiments. Compounds were dissolved in CH_3OH:H_2O 1:1 and the solvent evaporated afterward. 1–2 mg of the solids obtained were placed between two cover glasses, and heated up to their melting point on a hot plate (covered sample, Method A) the system was kept under heating several minutes after melting. To check the effect of the air on the thermal decomposition, experiments were also performed placing the sample on cover glasses and heating them up to their melting point (uncovered sample, Method B, heating at open air). Experiments were monitored by TLC, UV–Vis and ^{1}H-NMR spectroscopy and UV-LDI-MS.

Computational methods. DFT calculations were performed using the B3LYP exchange-correlation functional together with the standard 6-31++G(d,p) basis set. The stationary points were characterized by frequency calculations to verify that the transition structures had only one imaginary frequency. The solvent effects on the mechanism have been considered using a self-consistent reaction field method based on the Tomasi's polarizable continuum model. As the solvent used in the experimental work was CH_3CN, we have selected its dielectric constant ε = 37.5. Thermodynamic calculations were made with the standard statistical thermodynamics at 298.15 K and 1 atm. All calculations were carried out with the Gaussian09 suite of programs (15).

RESULTS

Spectroscopic and photophysical properties

Photophysical properties of the studied dihydroxyacetophenones were characterized by UV–Vis and fluorescence spectra, together with the quantum yield of fluorescence which was measured in CH_3CN.

UV–Vis spectra of dihydroxyacetophenones are characterized by the presence of two bands corresponding to a two π–π*, this assignation was based on TDDFT calculation (see Supplementary Materials). All the dihydroxyacetophenones show very week fluorescence as indicated by the very low fluorescence quantum yields measured (Table 1). This finding may be rationalized by operation of efficient excited-state intramolecular proton transfer (ESIPT) which lowers the fluorescence quantum yield Φ_f. This observation was previously reported for 2-hydroxyacethophenone (Fig. 2) (16). The most common acidic group in the ESIPT reactions is the phenolic OH, whereas the basic site is usually a heteroatom such as the carbonyl oxygen or nitrogen of a heterocycle.

However, an efficient intersystem crossing may also affect the fluorescence rendering the triplet state of the dihydroxyacetophenones. Thus, analysis of the Stokes shift must also be considered diagnostic for ESIPT reaction. Stokes shifts for the dihydroxyacetophenones are collected and shown in Table 1. 2,4-DHA shows the largest Stokes shift followed by 2,6-DHA, whereas 2,5-DHA shows a small shift of the fluorescence spectrum.

Photochemical stability

As UV-MALDI-MS experiments are generally performed at 355 nm, DHA acetonitrile solutions were irradiated first at 366 nm and also at 254 nm and $\lambda_{exc} > 300$ nm under air and nitrogen. No chemical changes were observed for 2,4, 2,5 and 2,6-DHA through TLC, ^{1}H-NMR and UV-LDI-MS. On the other hand, 3,5-DHA showed important decomposition (50% conversion) evidenced by the change in color, morphology and in the UV-LDI and ^{1}H-NMR spectra, yielding a brown polymeric product, which was not possible to purify (Fig. 3 for 2,4 and 3,4-DHA; see Supplementary Materials for the rest of dihydroxyacetophenones). UV–Vis spectral changes observed for 2,5 and 2,6-DHA with the absence of chemical changes could be attributed to a keto-enol tautomerization, which does not occur for 3,5-DHA.

Table 1. Spectral properties of dihydroxyacetophenones in CH_3CN.

	Absorption*	Emission		
	λ_{max} (log ε)	λ_{max}†	Φ_f‡	ν§
2,4-DHA	272 (4.26) 312 (3.9)	397	0.006	6800
2,5-DHA	254 (3.89) 359 (3.64)	396	0.004	2600
2,6-DHA	265 (3.86) 341 (3.53)	394	0.004	3900
3,5-DHA	263 (3.69) 320 (3.14)	400	0.008	6250

*Maximum of the absorption spectrum measured in nm; †Maximum of the fluorescence spectrum exciting at 355 nm; ‡Fluorescence quantum yields determined by use of quinine sulfate in 0.05 M aqueous H_2SO_4; λ_{exc} = 355 nm; §Stokes shift measured in cm^{-1}.

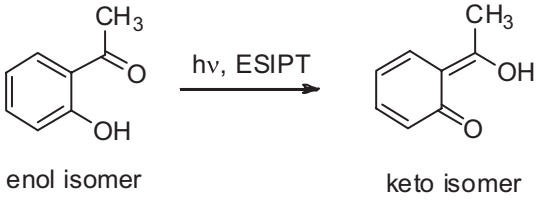

Figure 2. Excited-state intramolecular proton transfer for 2-hydroxyacetophenone.

Thermal stability

Dihydroxyacetophenones were heated up to their melting point as described in Materials and Methods section. Thermal stability experiments of the DHA crystalline matrices at their melting points were conducted by heating the selected powdered compound placed as a sandwich between two square microscope coverslips (thin windows of glass) on a heating block (Fisher-Johns apparatus) (Method A). To check the effect of air on the process the solid placed on a thin microscope glass coverslip was heated without covering (Method B). Except for a darkening of the melted product for 3,5-DHA, no changes were observed after heating the dihydroxyacetophenones. TLC analysis of the solid residue obtained after melting the matrix by method A using the commercial compound as reference clearly showed the same chromatographic behavior (identical aspect of the spots and F_r values) for all dihydroxyacetophenones. The UV-absorption spectra in CH_3CN of the melted matrix were registered and compared with those of the corresponding reference. The melted matrix showed identical absorption (shape of the bands, wavelength location, λ_{max}) to those of the starting material. Finally, the ^{1}H nuclear magnetic resonance (^{1}H-NMR) spectra obtained for the solid remaining after melting each matrix were identical to that of those corresponding nonmelted matrix. The same result was observed by UV-LDI-MS, where no signals at higher values of m/z were detected (see experimental data in Supplementary Materials).

Laser Flash Photolysis

Although LFP was performed for all the dihydroxyacetophenones under study, only 2,4-DHA gave rise a transient absorption with a maximum at 400 nm. The transient decayed with $k = 5.9 \pm 0.4 \times 10^4$ s^{-1} (lifetime of 17 $\pm$ 1 μs), and it was not affected by the oxygen concentration (Fig. 4a and b). This last observation ruled out the mediation of the triplet for the DHA. As previously mentioned, 2,4-DHA showed the largest Stokes shift in fluorescence and the transient observed may correspond to the keto isomer formed upon ESIPT reaction. To confirm the keto-enol nature of the intermediate observed by LFP, the effect of proton donors like water and alcohols was examined. Figure 5 illustrates the effect of the addition of water to the decay trace monitored at 400 nm.

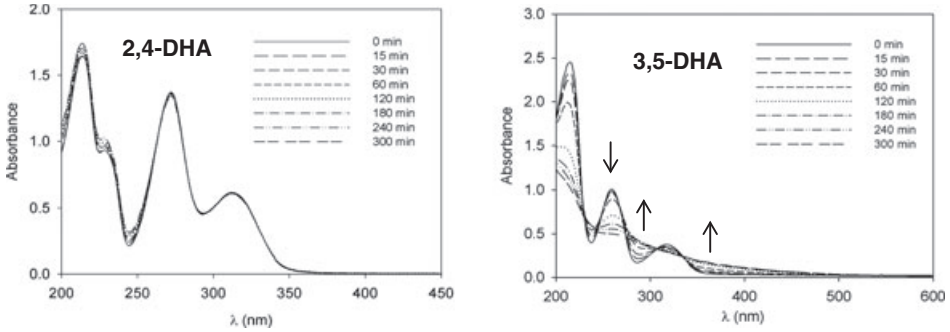

Figure 3. Irradiation of 2,4 and 3,5-DHA in acetonitrile solution at 254 nm under nitrogen atmosphere.

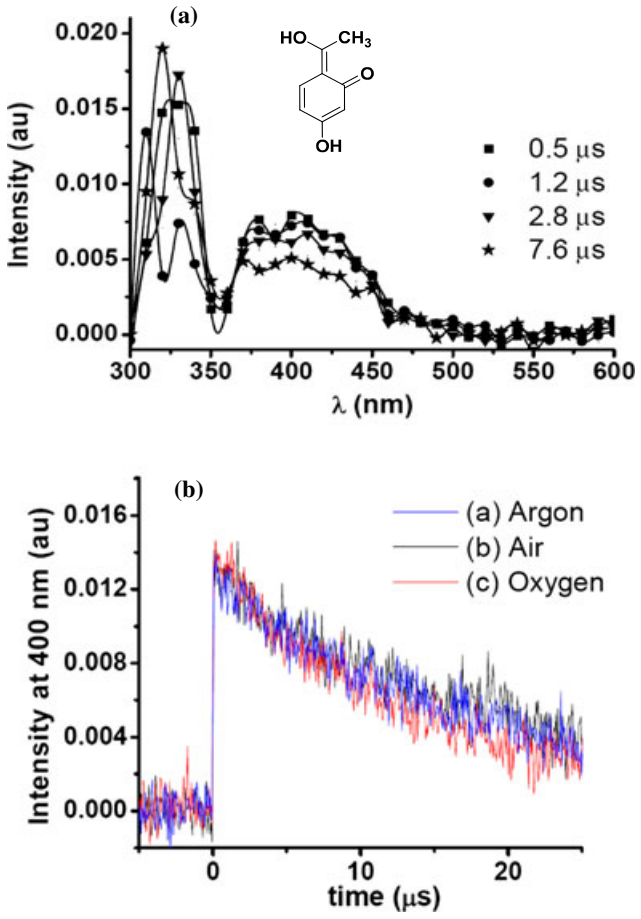

Figure 4. (a) Transient absorption spectrum of 2,4-DHA (3 mM) obtained by 355 nm laser photolysis in CH_3CN at 0.5 μs (■), 1.2 μs (●), 2.8 μs (▼) and 7.6 μs (*) after the laser pulse. (b) Time trace (monitoring at 400 nm) of the transient absorption spectrum of 2,4-DHA under (a) Argon, (b) aerated and (c) oxygen atmosphere.

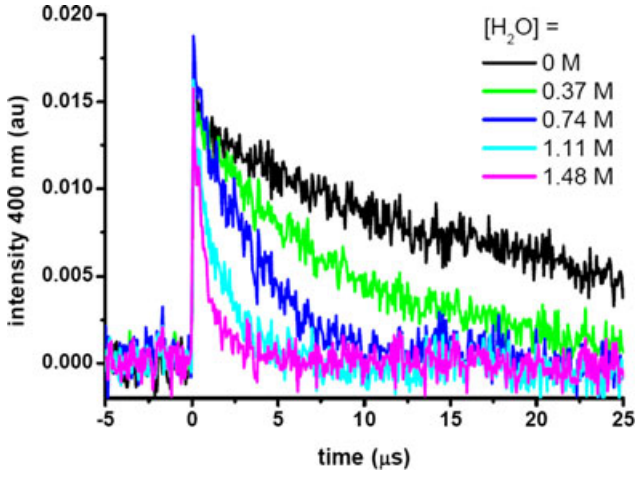

Figure 5. Decay kinetic monitored at 400 nm of the transient absorption spectrum of 2,4-DHA obtained by 355 nm laser photolysis in CH_3CN at different water concentration.

The effect of H_2O, D_2O, CH_3OH and CD_3OD and different alcohols on the decay rate of the transient was examined by measuring the decay rate at 400 nm as a function of the proton donor concentration in CH_3CN at 298 K. Figure 6 depicts the logarithmic plots of the observed decay rate (k_{obs}) against log[CH_3OH] or log[CD_3OD]. The linear nature of the log–log plot responds to Eq. (1), where the slope is the reaction order of the process for the R–OH, and the intercept is the log of the rate constant for the intermolecular reaction. In Table 2, the data obtained for all the proton donors studied yield a reaction order close to two for H_2O and D_2O, while for the alcohols this value ranges from 1.1 to 1.3. Therefore, more than one water or alcohol molecule are considered to participate in the catalyzed decay process. From Table 2 it is also possible to determine the isotope effect, where k^{H_2O}/k^{D_2O} and k^{CH_3OH}/k^{CD_3OD} are 2.7 and 2.8 respectively. This relatively large isotope effect at a 0.1 M concentration indicates the proton transfer nature of the reaction (17). This last observation, together with the low fluorescence quantum yield and the large Stokes shift, allows us to unambiguously assign the intermediate observed by LFP as the keto isomer formed by ESIPT as indicated in Fig. 7

$$\log k_{obs} = \log k^{ROH} + n \log [ROH] \quad (1)$$

DISCUSSION

Except for 3,5-DHA, all compounds showed high photochemical stability under irradiation. Starting compounds were recovered

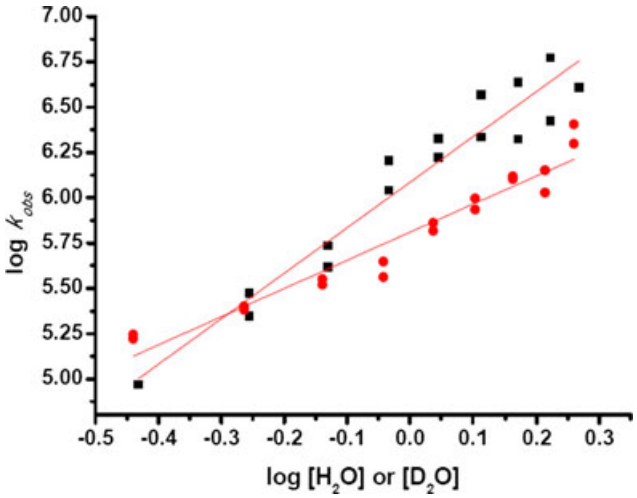

Figure 6. Effect of H_2O (■) or D_2O (●) on the observed decay rate (k_{obs}) monitored at 400 nm of the transient obtained by 355 nm laser photolysis of 2,4-DHA in CH_3CN at 293 K.

Table 2. Logarithm of rate constant and reaction order of the proton donors obtained by Eq. (1) of the transient absorption of 2,4-DHA measured at 400 nm in CH_3CN at 293 K.

Proton donor	log k	n
H_2O	6.22 ± 0.06	2.1 ± 0.2
D_2O	5.79 ± 0.03	2.0 ± 0.2
CH_3OH	5.47 ± 0.01	1.06 ± 0.05
CD_3OD	5.02 ± 0.06	1.1 ± 0.1
CH_3CH_2OH	5.48 ± 0.01	1.2 ± 0.1
Isopropanol	5.86 ± 0.01	1.2 ± 0.1
tert-butanol	5.54 ± 0.03	1.3 ± 0.2
1,3-propanediol	5.94 ± 0.02	1.2 ± 0.1

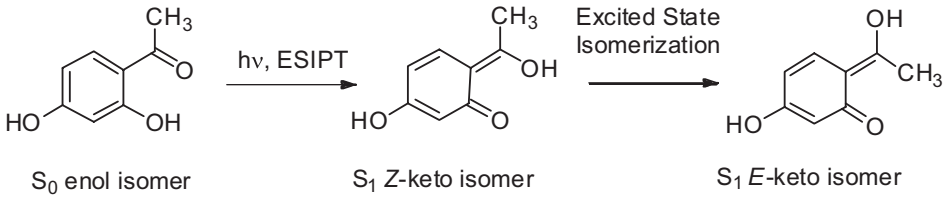

Figure 7. Excited-state intramolecular proton transfer for 2,4-DHA.

unchanged after several hours and the spectral changes of 2,4; 2,5 and 2,6-DHA may be attributed to a keto-enol tautomerization in the excited state. Thermal stability results shown previously suggest that their performance as UV-MALDI matrices is more related to their photochemical behavior.

All dihydroxyacetophenones showed very week fluorescence, with Φ_f in the order of 10^{-3} and none showed contribution of their triplet states in their photophysics properties as evidenced by the LFP study. It is well demonstrated that electronic excitation in systems like *o*-hydroxybenzaldehyde with a preexisting hydrogen bond in the ground-state results in a rapid proton translocation occurring in the first excited singlet state, through a process commonly known as ESIPT (18,19). Furthermore, ESIPT is known to be a very efficient nonradiative deactivation channel for intramolecular hydrogen-bonded compounds and occurs in ultrafast time scale (20,21). This process could be operating in the photophysics of the dihydroxyacetophenones under study; however, the signature for ESIPT is manifested by largely Stokes shifted emission (*ca* 10 000 cm^{-1}) given by the keto isomer. Only 2,4-DHA displayed a large Stokes shift, whereas 2,5- and 2,6-DHA showed a relatively small energy difference between the absorption and the emission, indicating that probably nondramatic changes in their geometries occurred in their excited states. Furthermore, the observation of the keto isomer for 2,4-DHA by LFP confirmed the ESIPT process for this dihydroxyacetophenone. The long lifetime of this intermediate allows us to rationalize it as the *E* isomer for the keto form indicated in Fig. 7. This intermediate returns to the ground state by rotation of the carbon–carbon enolic double bond to the *Z* isomer that collapses in a very fast proton transfer to the enol isomer. A schematic energy-level diagram of the overall process is illustrated in Fig. 8, where the rate constant (k_{PT}) of the ESIPT process is considered to be much larger than k_f and k_{nr}; therefore, the observed fluorescence from S_1 state comes from the *Z*-keto isomer. A similar schematic diagram has been proposed for 1-hydroxy-2-acetylnaphthalene, whose behavior is very similar to the herein reported for 2,4-DHA (17).

The reactivity of *E*-keto isomer of 2,4-DHA toward proton donors showed a relative large isotope effect of 2.8, indicating that the mutual proton transfer between the intermediate at the proton donor plays an important role in the catalytic process. All the alcohols measured were less reactive than water and their reactivity did not vary greatly, with an average value of 4.5×10^5 M^{-1} s^{-1} for the rate constant of the proton catalyzed *E-Z* ground-state isomerization reaction. This process was considered to follow a second-order rate law as the rate order for the alcohols was close to the unity for the alcohols measured (Table 2). For 2,5- and 2,6-DHA, neither triplet excited state nor keto isomer formed by ESIPT was observed. The lack of transient detection can be rationalized as an absence of ESIPT

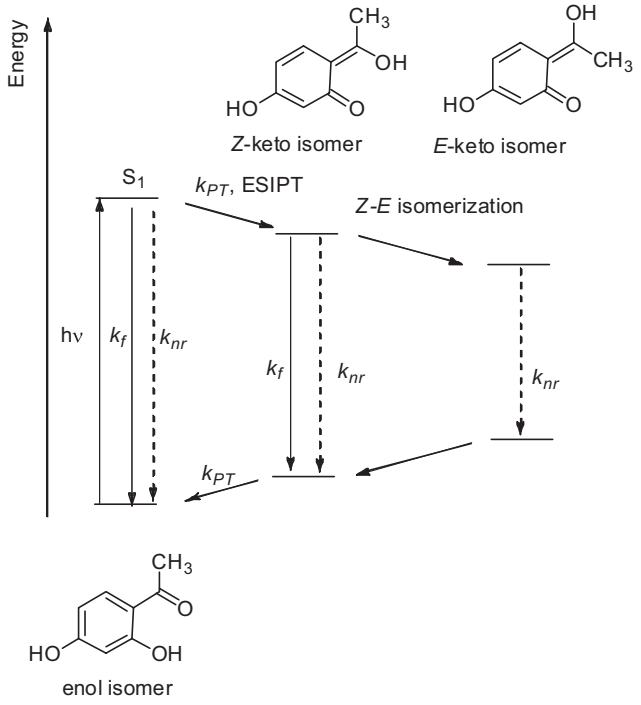

Figure 8. General energy-level diagram for 2,4-DHA.

reaction as the principal nonradiative decay channel; however, a further possibility is that the keto isomer is too unstable to be observed by our timescale LFP measurements. To gain insight into the dynamics of the proton translocation reaction, the ground-state intramolecular proton transfer (GSIPT) was explored for all the dihydroxyacetophenones by DFT quantum chemical calculation. Figure 9 compares the GSIPT curves for the dihydroxyacetophenones calculated by full optimization of the structure in acetonitrile. For each title molecule, the S_0 state potential energy profile along the reaction path shows two minima associated with the enol and the *E*-keto isomer. As expected by the dearomatization of the molecule, in all cases the *E*-keto isomer is less stable than the enol form. Furthermore, the transition state energy associated with the conversion between both conformers, starting from *E*-keto isomer and going to the enol, was calculated following the order 2,6-DHA (23.6 kcal mol^{-1}) < 2,4-DHA (24.6 kcal mol^{-1}) ≈ 2,5-DHA (24.7 kcal mol^{-1}). These results for 2,5- and 2,6-DHA suggest that, if *E*-keto isomers are formed upon photoexcitation, they would have similar lifetimes as the energies associated with the proton translocation are similar among the dihydroxyacetophenones. Most likely, ESIPT reactions never take place for 2,5 and 2,6-DHA as the energy difference between absorption and emission is too narrow to allow

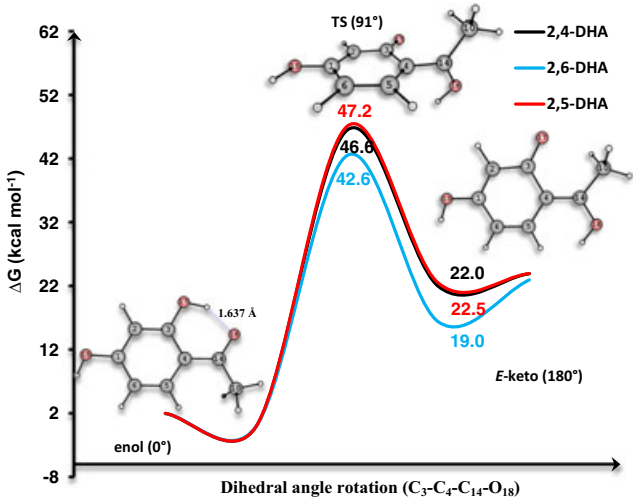

Figure 9. B3LYP/6-31++G(d,p) relative energies (kcal mol^{-1}), in acetonitrile, associated with the transition states for the ground-state intramolecular proton transfer between the enol and keto isomers for dihydroxyacetophenones.

proton transfer in the excited state (Stokes shifts are 2600 cm^{-1} for 2,5-DHA and 3900 cm^{-1} for 2,6-DHA). In addition, it is well known that substitution at *para* position with respect to the phenolic OH group showed strong suppression of excited-state proton dislocation as reported for 5-amino and 5-methoxysalicylic acid (22). Most likely, the excited-state *Z-E* keto isomerisation cannot be displayed because of the presence of a very shallow excited-state surface with the *Z*-keto isomer as the single minimum. This could account for the absence of ESIPT for 2,5-DHA, where the OH at the five positions reduces the acidity of the hydroxyl group in the excited state, whereas OH at the four and six positions would increase the basicity of the carbonyl group, therefore facilitating the ESIPT reaction observed for 2,4-DHA but not for 2,6-DHA. To provide a better explanation of these phenomena, a complete exploration of the ESIPT surface using time-dependent density functional theory (TDDFT) must be considered. However, this is beyond the scope of this work where the quality of a material as UV-MALDI-MS matrices is rationalized in terms of its photophysical properties.

CONCLUSIONS

In the case of 3,5-DHA, this is the first attempt of its use as a UV-MALDI-MS matrix. The absence of phototautomerization for this compound could explain the lack of photostability observed in our experimental conditions. The other three dihydroxyacetophenones showed thermal and photochemical stability when irradiated with different UV sources (lamps and lasers; LFP, UV-LDI-MS). As they also showed very low fluorescence quantum yields, their main deactivation mechanism may involve heat emission. 2,4-DHA has an ESIPT yielding a detectable transient through LFP, whereas 2,5 and 2,6-DHA might generate less stable keto photoisomers.

Acknowledgements—This work has been supported in part by Consejo Nacional de Investigaciones Científicas y Técnicas (CONICET, PIP 00264 and PIP 0400), Universidad de Buenos Aires (X088), Secretaría de Ciencia y Tecnología, Universidad Nacional de Córdoba and Fondo para la Investigación Científica y Tecnológica Argentina.

UV-MALDI-TOF/TOF-MS was performed using CEQUIBIEM (FCEN-UBA) facilities (ANPCyT, PME 125). R.E-B, O.I.T and J.E.A are research members of CONICET. G.O-M. gratefully acknowledges receipt of fellowship from CONICET.

SUPPORTING INFORMATION

Additional Supporting Information may be found in the online version of this article:

Figure S1. UV-MALDI mass spectra of 1^F-fructofuranosylnystose (A, PM 828.28 Da). Positive ion mode (a) and negative ion mode (b), matrices: dihydroxyacetophenones as indicated.

Figure S2. Photochemical stability of dihydroxyacetophenones. UV–Vis absorption spectra of dihydroxyacetophenones at 254, 366 and $\lambda > 300$ nm (solvent: CH_3CN).

Figure S3. ^{1}H-NMR (200 MHz) spectra of dihydroxyacetophenones, before and after irradiation (solvent CD_3OD).

Figure S4. UV-LDI mass spectra of 3,5-DHA (M, m. w. 152.088 Da), before and after irradiation. Positive ion mode.

Figure S5. Thermal treatment of dihydroxyacetophenones. UV–Vis absorption spectra of dihydroxyacetophenones and melted dihydroxyacetophenones (Methods A and B) (solvent: CH_3CN).

Figure S6. Thermal treatment of dihydroxyacetophenones. ^{1}H-NMR (200 MHz) spectra of dihydroxyacetophenones and melted dihydroxyacetophenones (solvent CD_3OD).

Figure S7. UV-LDI mass spectra of 3,5-DHA (M, m. w. 152.088 Da) and melted 3,5-DHA. Positive ion mode.

Figure S8. Representative electronic transitions for 2,4-DHA computed by TDDFT at the B3LYP with 6-31++G(d,p) basis set.

Table S1. Transition state energy associated with the GSIPT from *E*-keto isomer to the enol form.

REFERENCES

1. Mohr, M. D., K. O. Börnsen and H. M. Widmer (1995) Matrix-assisted laser desorption/ionization mass spectrometry: improved matrix for oligosaccharides. *Rapid Commun. Mass Spectrom.* **9**, 809–814.
2. Krause, J., M. Stoeckli and U. P. Schlunegger (1996) Studies on the selection of new matrices for ultraviolet matrix-assisted laser desorption/ionization time-of-flight mass spectrometry. *Rapid Commun. Mass Spectrom.* **10**, 1927–1933.
3. Zaia, J. (2004) Mass spectrometry of oligosaccharides. *Mass Spectrom. Rev.* **23**, 161–227.
4. Harvey, D. J. (2012) Analysis of carbohydrates and glycoconjugates by matrix-assisted laser desorption/ionization mass spectrometry: an update for 2007–2008. *Mass Spectrom. Rev.* **31**, 183–311.
5. Weller, A. (1961) Fast reactions of excited molecules. *Prog. React. Kinet.* **1**, 187–214.
6. Herek, J. L., S. Pedersen, L. Banares and A. H. Zewail (1992) Femtosecond real-time probing of reactions. IX. Hydrogen-atom transfer. *J. Chem. Phys.* **97**, 9046–9061.
7. Le Gourrierec, D., S. M. Ormson and R. G. Brown (1994) Excited state intramolecular proton transfer. Part 2. ESIPT to oxygen. *Prog. React. Kinet.* **19**, 211–275.
8. Lüdemann, H.-C., F. Hillenkamp and R. W. Redmond (2000) Photoinduced hydrogen atom transfer in salicylic acid derivatives used as matrix-assisted laser desorption/ionization (MALDI) matrices. *J. Phys. Chem.* **104**, 3884–3893.
9. Ehring, H., C. Costa, P. A. Demirev and B. U. R. Sundqvist (1996) Photochemical vs thermal mechanisms in matrix-assisted laser desorption/ionization probed by back side desorption. *Rapid Commun. Mass Spectrom.* **10**, 821–824.

10. Ehring, H. and B. U. R. Sundqvist (1995) Excited state relaxation processes of MALDI-matrices studied by luminescence spectroscopy. *J. Mass Spectrom.* **30**, 1301–1310.
11. Harvey, D. H. (2006) Analysis of carbohydrates and glycoconjugates by matrix-assisted laser desorption/ionization mass spectrometry: an update covering the period 1999–2000. *Mass Spectrom. Rev.* **25**, 595–662.
12. Tarzi, O. I., H. Nonami and R. Erra-Balsells (2009) The effect of temperature on the stability of compounds used as UV-MALDI-MS matrix: 2,5-dihydroxybenzoic acid, 2,4,6-trihydroxyacetophenone, α-cyano-4-hydroxycinnamic acid, 3,5-dimethoxy-4-hydroxycinnamic acid, nor-harmane and harmane. *J. Mass Spectrom.* **44**, 260–277.
13. Miller, J. N. (ed.) (1981) *Standards in Fluorescence Spectroscopy*. Chapman and Hall Ltd., London, UK.
14. Murov, S. L., I. Carmichael and G. L. Hung (1993) *Handbook of Photochemistry*, 2nd edn. Marcel Dekker, New York.
15. Frisch, M. J., G. W. Trucks, H. B. Schlegel, G. E. Scuseria, M. A. Robb, J. R. Cheeseman, G. Scalmani, V. Barone, B. Mennucci, G. A. Petersson, H. Nakatsuji, M. Caricato, X. Li, H. P. Hratchian, A. F. Izmaylov, J. Bloino, G. Zheng, J. L. Sonnenberg, M. Hada, M. Ehara, K. Toyota, R. Fukuda, J. Hasegawa, M. Ishida, T. Nakajima, Y. Honda, O. Kitao, H. Nakai, T. Vreven Jr., J. A. Montgomery, J. E. Peralta, F. Ogliaro, M. Bearpark, J. J. Heyd, E. Brothers, K. N. Kudin, V. N. Staroverov, R. Kobayashi, J. Normand, J. K. Raghavachari, A. Rendell, J. C. Burant, S. S. Iyengar, J. Tomasi, M. Cossi, N. Rega, N. J. Millam, M. Klene, J. E. Knox, J. B. Cross, V. Bakken, C. Adamo, J. Jaramillo, R. Gomperts, R. E. Stratmann, O. Yazyev, A. J. Austin, R. Cammi, C. Pomelli, J. W. Ochterski, R. L. Martin, K. Morokuma, V. G. Zakrzewski, G. A. Voth, P. Salvador, J. J. Dannenberg, S. Dapprich, A. D. Daniels, Ö. Farkas, J. B. Foresman, J. V. Ortiz, J. Cioslowski and D. J. Fox, (2009) *GAUSSIAN 09 (Revision A.1)*, Gaussian, Inc., Wallingford, CT.
16. Nisbiya, T. S., N. Yamauchi, M. B. Hirota and I. H-nazaki (1986) Fluorescence studies of the intramolecularly hydrogen-bonded molecules o-hydroxyacetophenone and salicylamide and related molecules. *J. Phys. Chem.* **90**, 5730–5735.
17. Tobita, S., M. Yamamoto, N. Kurahayashi, R. Tsukagoshi, Y. Nakamura and H. Shizuka (1998) Effect of electronic structure on the excited-state intramolecular proton transfer of 1-hydroxy-2-acetonaphthone and related compounds. *J. Phys. Chem. A* **102**, 5206–5214.
18. Barbara, P. F., L. E. Walsh and L. E. Brus (1989) Picosecond kinetic and vibrationally resolved spectroscopic studies of intramolecular excited-state hydrogen atom transfer. *J. Phys. Chem.* **98**, 29–34.
19. Douhal, A., F. Lahrnani and A. H. Zewail (1996) Proton-transfer reaction dynamics. *Chem. Phys.* **207**, 477–498.
20. Lochbrunner, S., A. J. Wurzer and E. Riedle (2003) Microscopic mechanism of ultrafast excited-state intramolecular proton transfer: a 30-fs study of 2-(2′-Hydroxyphenyl)benzothiazole. *J. Phys. Chem. A* **107**, 10580–10590.
21. Mitra, A., T. S. Singh, A. Mandal and S. Mukherjee (2007) Experimental and computational study on photophysical properties of substituted *o*-hydroxy acetophenone derivatives: intramolecular proton transfer and solvent effect. *Chem. Phys.* **342**, 309–317.
22. Jang, S., S. Jin II and C. R. Park (2007) TDDFT potential energy functions for excited state intramolecular proton transfer of salicylic acid, 3-aminosalicylic acid, 5-aminosalicylic acid, and 5-methoxysalicylic acid. *Bull. Korean Chem. Soc*. **28**, 2343–2353.